Mitochondrial Localization and Regulation of $BRAF^{V600E}$ in Thyroid Cancer: A Clinically Used RAF Inhibitor Is Unable to Block the Mitochondrial Activities of $BRAF^{V600E}$

Min Hee Lee, Seong Eun Lee, Dong Wook Kim, Min Jeong Ryu, Sung Jin Kim, Sung Joong Kim, Yong Kyoung Kim, Ji Hoon Park, Gi Ryang Kweon, Jin Man Kim, Jung Uee Lee, Valentina De Falco, Young Suk Jo, and Minho Shong

Departments of Internal Medicine (M.H.L., S.E.L., D.W.K., M.J.R., S.Jin.K., S.Joong.K., Y.K.K., Y.S.J., M.S.), Biochemistry (J.H.P., G.R.K.), and Pathology (J.M.K.), Laboratory of Endocrine Cell Biology, Division of Endocrinology, Chungnam National University School of Medicine, Jung-gu Daejeon 301-721, Korea; Department of Pathology (J.U.L.), Daejeon St. Mary's Hospital, The Catholic University of Korea, Jung-gu Daejeon 301-723, Korea; and Dipartimento di Biologia e Patologia Cellulare e Molecolare (V.D.F.), Universitá Federico II/Istituto di Endocrinologia e Oncologia Sperimentale Consiglio Nazionale delle Ricerche, 80131 Napoli, Italy

Context: The oncogenic $BRAF^{V600E}$ mutation results in an active structural conformation characterized by greatly elevated ERK activity. However, additional cellular effects caused by subcellular action of $BRAF^{V600E}$ remain to be identified.

Objective: To explore these effects, differences in the subcellular localization of wild-type and mutant BRAF in thyroid cancer were investigated.

Results: A significant proportion of endogenous and exogenous $BRAF^{V600E}$, but not wild-type BRAF, was detected in the mitochondrial fraction, similar to other BRAF mutants including $BRAF^{V600D}$, $BRAF^{V600K}$, $BRAF^{V600R}$, and $BRAF^{G469A}$, which showed elevated kinase activity and mitochondrial localization. Induced expression of $BRAF^{V600E}$ suppressed the apoptotic responses against staurosporine and TNFα/cycloheximide. Interestingly, the mitochondrial localization and antiapoptotic activities of $BRAF^{V600E}$ were unaffected by sorafenib and U0126 suppression of MAPK kinase (MEK) and ERK activities. Similarly, although the RAF inhibitor sorafenib effectively inhibited MEK/ERK activation, it did not block the mitochondrial localization of $BRAF^{V600E}$. In addition, inducible expression of $BRAF^{V600E}$ increased the glucose uptake rate and decreased O_2 consumption, suggesting that $BRAF^{V600E}$ reduces mitochondrial oxidative phosphorylation, a signature feature of cancer cells. Again, these metabolic alterations resulted by $BRAF^{V600E}$ expression were not affected by the treatment of thyroid cells by sorafenib. Therefore, RAF and MEK inhibitors are unable to block the antiapoptotic activity of $BRAF^{V600E}$ or correct the high glucose uptake rate and glycolytic activity and suppressed mitochondrial oxidative phosphorylation induced by $BRAF^{V600E}$.

Conclusions: The mitochondrial localization observed in oncogenic BRAF mutants might be related to their altered responses to apoptotic stimuli and characteristic metabolic phenotypes found in thyroid cancer. The inability of MEK and RAF inhibitors, U0126 and sorafenib, respectively, to block the mitochondrial localization of $BRAF^{V600E}$ has additional therapeutic implications for $BRAF^{V600E}$-positive thyroid cancers. **(*J Clin Endocrinol Metab* 96: E19–E30, 2011)**

ISSN Print 0021-972X ISSN Online 1945-7197
Printed in U.S.A.

doi: 10.1210/jc.2010-1071 Received May 10, 2010. Accepted September 7, 2010.
First Published Online October 6, 2010

Abbreviations: Bad, Bcl-2-associated death promoter; Bcl-2, B-Cell lymphoma 2; Bim, Bcl-2 interacting mediator of cell death; CHX, cycloheximide; HIF, hypoxia-inducible factor; MEK, MAPK kinase; MST1, mammalian STE20-like kinase 1; MTS, mitochondrial matrix target sequences; PARP, poly [ADP-ribose] polymerase 1; PTC, papillary thyroid cancer; STS, staurosporine; TOM40, translocase of outer mitochondrial membrane 40.

The most frequently observed BRAF mutation in thyroid cancer is the V600E mutant (BRAF^{V600E}), which exhibits greatly elevated kinase activity. This altered form of BRAF constitutively stimulates ERK activity and generates invasive papillary thyroid cancer (PTC) *in vivo* (1–4). The structural basis for this constitutive activation by BRAF^{V600E} is explained by its active conformation, which mimics phosphorylation of the activation segment of the BRAF protein (5). This active conformation of BRAF^{V600E} confers the ability to phosphorylate MAPK kinase (MEK) 1/2, which in turn phosphorylates tyrosine/threonine residues in ERK1/2. Upon activation, the ERKs activate nuclear transcription factors that are implicated in cell growth, differentiation, survival, and tumor behavior (3, 6). Based on these findings, ERK signaling pathways have become the primary therapeutic targets for BRAF^{V600E}-positive PTC.

The first generation of RAF inhibitors (*e.g.* sorafenib) has shown limited efficacy, failing to induce complete remission in advanced tumors, such as melanoma and PTC, which have a high incidence of BRAF mutations (7–9). Furthermore, MEK inhibitors have not achieved major clinical results in advanced cancers (10, 11). The relatively modest clinical efficacy of these inhibitors on BRAF^{V600E}-positive cancers remains to be explained. In addition to the failure of these inhibitors to inhibit sufficiently RAF and ERK kinases in clinically advanced tumors, RAF inhibitors could also promote paradoxical CRAF activation by BRAF, as recently reported (12–14). In addition, BRAF^{V600E} has mutation-specific effects that are related to tumor behavior but that are ERK independent. The ERK-independent effects of BRAF^{V600E}, which are poorly understood (15), have been suggested by several lines of circumstantial evidence to be responsible for determining tumor characteristics. For example, some tumor cell lines that express BRAF^{V600E} did not show inhibition of the S phase by a MEK inhibitor (1). Furthermore, other tumor-specific characteristics, such as enhanced glycolysis and suppressed mitochondrial functions, have not been clearly shown to be induced by BRAF^{V600E}-ERK pathways (16, 17). These findings underscore the need to identify the ERK-independent effects of BRAF^{V600E} to develop better drugs to treat BRAF^{V600E}-positive PTC.

The findings of the present study show that BRAF^{V600E} interacts with mitochondria via an ERK-independent, mutation-specific mitochondrial localization. The mitochondrial localization of BRAF^{V600E} generated antiapoptotic effects and metabolic changes characterized by decreased O_2 consumption and an increased rate of glucose uptake, suggesting reduced mitochondrial oxidative phosphorylation. Surprisingly, clinically used and well-known RAF inhibitor had no effect on the mitochondrial interactions or activities of BRAF^{V600E}. These new insights into the mutation-specific roles played by BRAF^{V600E} may be important for the development of future therapeutics.

Materials and Methods

Materials

Cell culture reagents were purchased from Life Technologies Inc. (Gaithersburg, MD), Sigma Chemical Co. (St. Louis, MO), Fisher Scientific (Fairlawn, NJ), and Corning Inc. (Corning, NJ). U0126 and TNFα were purchased from Calbiochem (San Diego, CA). Doxycycline, staurosporine, and cycloheximide were purchased from Sigma Aldrich Inc. BAY43–9006 (sorafenib) was kindly provided by Bayer Schering Pharma AG (Berlin, Germany). The following antibodies were used: anti-BRAF (F-7), antitransporter of outer membrane (TOM)-40 (Santa Cruz Biotechnology, Santa Cruz, CA), anti-cytochrome *c* (BD Bioscience, San Jose, CA), anti-p44/p42 MAPK, anti-phospho-p44/42 MAPK (Thr202/Tyr204), anti-B-cell lymphoma 2 (Bcl-2)-interacting mediator of cell death (Bim), anti-poly(ADP-ribose) polymerase (PARP), anti-Myc-Tag (9B11), and the apoptosis sampler kit (Cell Signaling Technology, Beverly, MA). pEFm-BRAF^{WT}, -BRAF^{V600E}, -BRAF^{V600D}, -BRAF^{V600R}, and -BRAF^{V600K} were kindly provided by Dr. Marais and Dr. Hayward (Institute of Cancer Research, London, UK). pEFm-BRAF^{G469A} and -BRAF^{G596R} were obtained from pEFm-BRAF^{WT} by site-directed mutagenesis using the QuickChange XL mutagenesis kit (Stratagene, La Jolla, CA) (18).

Cell culture, transfection, and Tg-BRAF^{V600E} mice

$PCCl_3$ cells with doxycycline-inducible expression of BRAF^{V600E} were kindly donated by Dr. James A. Fagin (Memorial Sloan Kettering Cancer Center, New York, NY). HeLa cells containing the doxycycline-inducible BRAF^{WT} or BRAF^{V600E} systems were generated using the ViraPower lentiviral expression systems and ViraPower T-REX lentiviral gateway vector kit (Invitrogen, Carlsbad, CA). Primary cultured cells originating from normal thyroid and BRAF^{V600E}-positive PTC (PTC-BRAF^{V600E}) were prepared by proteolytic digestion and mechanical disaggregation. For this experiment, we isolated thyroid cancer cells from three different patients with classic papillary thyroid tumors harboring BRAF^{V600E}, the presence of which was confirmed in fine-needle aspiration samples before operation. All protocols using the human thyroid cells and related studies were approved by Institutional Review Board of the Chungnam National University School of Medicine.

$PCCl_3$ and primary culture cells were grown in 6H5 media with previously described methods (19). $PCCl_3$ cells were transiently transfected with pEFm-BRAF^{WT}, BRAF^{V600E}, BRAF^{V600D}, BRAF^{V600R}, BRAF^{V600K}, BRAF^{G469A}, and BRAF^{G596R} using Lipofectamine PLUS (Invitrogen).

Tg-BRAF^{V600E} mice were kindly provided by Dr. James A. Fagin (Memorial Sloan Kettering Cancer Center) (20). All animal procedures were in accordance with the guidelines of the Institutional Animal Care and Use Committee of the Chungnam National University School of Medicine.

Immunofluorescence staining

Cells were grown on coverslips in six-well plates and treated with MitoTracker (Molecular Probes Inc., Eugene, OR). After

incubation for 30 min under the specified growth conditions, cells were washed with 1× PBS and then fixed in 3.7% paraformaldehyde for 15 min at room temperature. Permeabilized cells were blocked with 1% BSA in 1× PBS for 45 min at room temperature. In the case of thyroid tissues isolated from Tg-BRAF^{V600E} mice, cryostat sections of 4 μm were collected on poly-L-lysine coated (0.1%) glass slides and fixed in 4% paraformaldehyde. Sections were blocked for 3 h in 5% BSA in PBS. Cells and tissues were incubated with primary antibody overnight at 4C, washed three times with 1× PBS, and incubated at 37 C for 1 h with secondary antibodies: fluorescein isothiocyanate-conjugated pure goat antimouse IgG and rhodamine (tetramethylrhodamine isothiocyanate)-conjugated pure goat antirabbit IgG (Jackson ImmunoResearch Laboratories Inc., West Grove, PA). Cells on coverslips and tissues on glass slides were mounted and observed using a laser-scanning confocal microscope (Olympus Corp., Lake Success, NY). To obtain tissue samples from the same sites, the thawed frozen tissues were embedded in paraffin and used for hematoxylin and eosin staining.

4,6-Diamidino-2-phenylindole staining

HeLa-BRAF^{WT} and HeLa-BRAF^{V600E} were treated with 1 μM doxycycline for 24 h, followed by staurosporine (1 μM) treatment for 4 h. Cells were washed, fixed in 4% formaldehyde, and then stained with (10 μL/reaction) in 1× PBS (10 mL) for 10 min at room temperature in the dark. The stained cells were observed under a fluorescence microscope.

Subcellular fractionation

HeLa-BRAF^{WT}, HeLa-BRAF^{V600E}, and PTC-BRAF^{V600E} were grown in 150-mm dishes. HeLa cells were treated with doxycycline, staurosporine, U0126, and sorafenib, according to the experimental design. After treatment, cells were washed with 1× PBS and harvested using 1× trypsin/EDTA solution. Cells were centrifuged at 1300 × *g* for 10 min at 4 C and then resuspended in 10 mM NaCl, 1.5 mM $MgCl_2$, 10 mM Tris-Cl (pH 7.5), and protease inhibitor. Cells were incubated for 5 min on ice to swell, homogenized on ice with a Teflon-glass Potter-Elvehjem homogenizer, and then centrifuged at 1300 × *g* for 10 min at 4 C. The supernatant was recentrifuged at 1500 × *g* for 15 min at 4 C, and then the final supernatant was used in sucrose gradient ultracentrifugation to purify the mitochondria. The pellet was resuspended in radioimmunoprecipitation assay buffer [50 mM Tris-HCl (pH 7.4), 4 mM EDTA, 6 mM NaCl, 5 mL Nonidet P-40, 0.25% Na-deoxycholate, and protease inhibitor], and sequential digestion was performed by treatment with proteinase K (50 μg/ml) in radioimmunoprecipitation assay buffer for the times indicated.

Immunoblot analysis

Whole-cell extracts, mitochondrial fractions, or cytoplasmic proteins were added to the sodium dodecyl sulfate sample buffer and denatured by boiling for 5 min. Proteins were separated by 8–15% SDS-PAGE and then transferred to a nitrocellulose membrane (GE/Amersham Biosciences, Cardiff, UK). After blocking, the blots were incubated with primary antibody in diluted blocking buffer overnight at 4 C and developed using a horseradish peroxidase-conjugated secondary antibody (Phototope-HRP Western blot detection kit; New England Biolabs, Ipswich, MA).

Measurement of O_2 consumption, glucose uptake, and ATP generation

O_2 consumption, 2-deoxyglucose uptake, and ATP generation were investigated using PC-BRAF^{WT} and PC-BRAF^{V600E}. O_2 consumption was determined using the oxygen-sensitive fluorophore in the BD Oxygen Biosensor System (BD Biosciences, Bedford, MA) and a Fluoroskan Ascent (Thermo Electron Corp., Vantaa, Finland). The glucose uptake assay was performed as follows. Cells were washed twice with Krebs-Ringer-phosphate-HEPES buffer [20 mM HEPES (pH 7.4), 5 mM KH_2PO_4, 1 mM $MgSO_4$, 1 mM $CaCl_2$, 136 mM NaCl, and 4.7 mM KCl] and then incubated in Krebs-Ringer-phosphate-HEPES buffer containing 1 μCi/ml deoxyglucose for 2 h at 37 C in 5% CO_2. After incubation, the cells were washed, and then 500 μl 0.2 M NaOH and 500 μl scintillation cocktail were added. Radioactivity levels were determined using a Beckman LS6500 scintillation counter (Beckman Instruments, Fullerton, CA). The relative ATP concentration was measured using the ATPlite one-step kit (Perkin-Elmer, Boston, MA), and the luminescence was measured using a Luminoskan Ascent (Thermo Labsystems, Helsinki, Finland).

Results

BRAF^{V600E} localizes to the outer membrane of mitochondria

Cancer cells show strong resistance to mitochondrial-mediated apoptosis and metabolic imbalances, exhibiting enhanced glycolysis and suppressed mitochondrial energy production (16, 17). The present electron microscopic data revealed that mitochondria of PTC-BRAF^{V600E} were mostly oval in form, whereas mitochondria of normal follicular cells were rod-like. Furthermore, in PTC-BRAF^{V600E} there was a reduction in the amount of electron dense materials, indicating partial loss of cristae structure (Supplemental Fig. 1, published on The Endocrine Society's Journals Online web site at http://jcem.endojournals.org). These mitochondrial morphological features of PTC-BRAF^{V600E} suggested decreased mitochondrial energy production and implied that BRAF^{V600E} may act directly on mitochondria to regulate mitochondrial function.

BRAF^{V600E} localization was analyzed by isolating mitochondrial fractions from PTC-BRAF^{V600E} (Supplemental Fig. 2). Interestingly, BRAF^{V600E} was found in both the soluble cytosolic and mitochondrial fractions (Fig. 1A, *left panel*), whereas wild-type BRAF was not detected in the mitochondrial fractions prepared from normal thyroid cells. These observations indicate that mutant BRAF^{V600E}, but not wild-type BRAF, interacts directly with mitochondria. To determine whether BRAF^{WT} and BRAF^{V600E} differ in their mitochondrial localization, soluble cytosolic and mitochondrial fractions were isolated from $PCCl_3$ thyroid cell lines, which express these proteins in a doxycycline-inducible manner (PC-BRAF^{WT} and PC-BRAF^{V600E}, respectively). Interestingly, inducible expression of BRAF^{V600E} also caused the loss of cristae structure in mitochondria

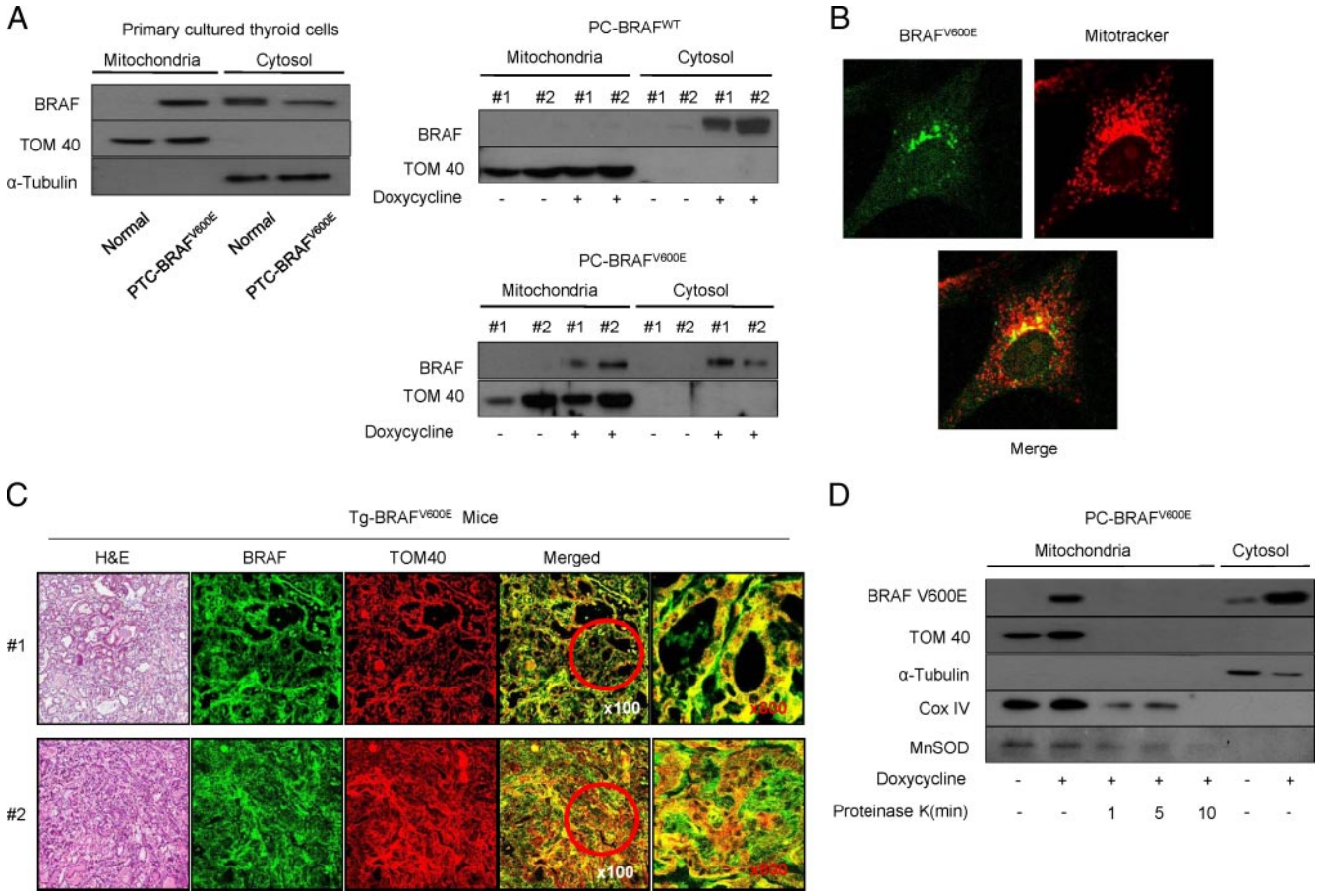

FIG. 1. Mitochondrial translocation of BRAF^{V600E}. A, Primary culture cells from BRAF^{V600E}-positive PTC (PTC-BRAF^{V600E}) and normal thyroid tissue (normal) were prepared for subcellular fractionation (*left panel*), as described in *Materials and Methods*. The markers, TOM40 and α-tubulin, were used to verify the identity and purity of the mitochondrial and cytosolic fractions, respectively. Based on these markers, a good overall yield was obtained without mixing of the fractions. PC-BRAF^{WT} and PC-BRAF^{V600E} were also prepared for subcellular fractionation (*right panel*). PC-BRAF^{WT} and PC-BRAF^{V600E} showed low basal BRAF expression and marked induction after 48 h of 1 μg doxycycline treatment. B, PTC-BRAF^{V600E} cells were fixed and processed for immunofluorescence staining of BRAF (*green fluorescence*) and mitochondria (MitoTracker, *red fluorescence*). C, Thyroid tissue obtained from TgBRAF^{V600E} mice was fixed and processed for immunofluorescence staining of BRAF (*green fluorescence*) and TOM40 (*red fluorescence*). D, Lysates of PC-BRAF^{V600E} cells treated with doxycycline for 48 h were digested sequentially with proteinase K after subcellular fractionation and immunoblots were used to examine the subcellular location of BRAF^{V600E}. The inner membrane protein cytochrome c oxidase subunit IV (CoxIV) and matrix protein manganese superoxide dismutase (MnSOD) were used as additional markers.

(Supplemental Fig. 3). Furthermore, BRAF^{V600E}, but not BRAF^{WT}, was detected consistently in the mitochondrial fractions of two cell lines obtained from different clones (Fig. 1A, *right panel*).

To visualize the endogenous mitochondrial localization of BRAF^{V600E}, immunofluorescence studies were performed using an anti-BRAF antibody to stain mutant BRAF proteins in PTC-BRAF^{V600E} and in the thyroid-specific BRAF^{V600E} transgenic mouse (Tg-BRAF^{V600E} mouse). As shown in Fig. 1B, a significant portion of BRAF^{V600E} colocalized with mitochondria in PTC-BRAF^{V600E}. In Tg-BRAF^{V600E} mice, BRAF immunoreactivity also colocalized with TOM40 in follicular cells (Fig. 1C, *upper panel*). In dedifferentiated, spindle-shaped cancer cells in Tg-BRAF^{V600E} mice, colocalization of BRAF with TOM40 was detected persistently (Fig. 1C, *lower panel*). In this experiment, we performed immunofluorescence staining using fluorescent-labeled secondary antibodies without primary antibody to evaluate interference from the nonspecific fluorescence of the fixed tissues. Major nonspecific fluorescence was observed in fibrous tissue, but follicular cells did not show significant nonspecific and autofluorescence that interferes with data interpretation (Supplemental Fig. 4).

Experiments were subsequently performed to investigate the mitochondrial compartment that directly interacts with mutant BRAF^{V600E}. Because BRAF has no obvious N-terminal mitochondrial matrix target sequences (MTS) (21), mutant BRAF may presumably be associated with the mitochondrial outer membrane. To define the localization of BRAF^{V600E} to a specific mitochondrial compartment, a sequential proteinase K digestion was performed on mitochondria purified from BRAF^{V600E}-containing cells (Fig. 1D). Evaluation of the

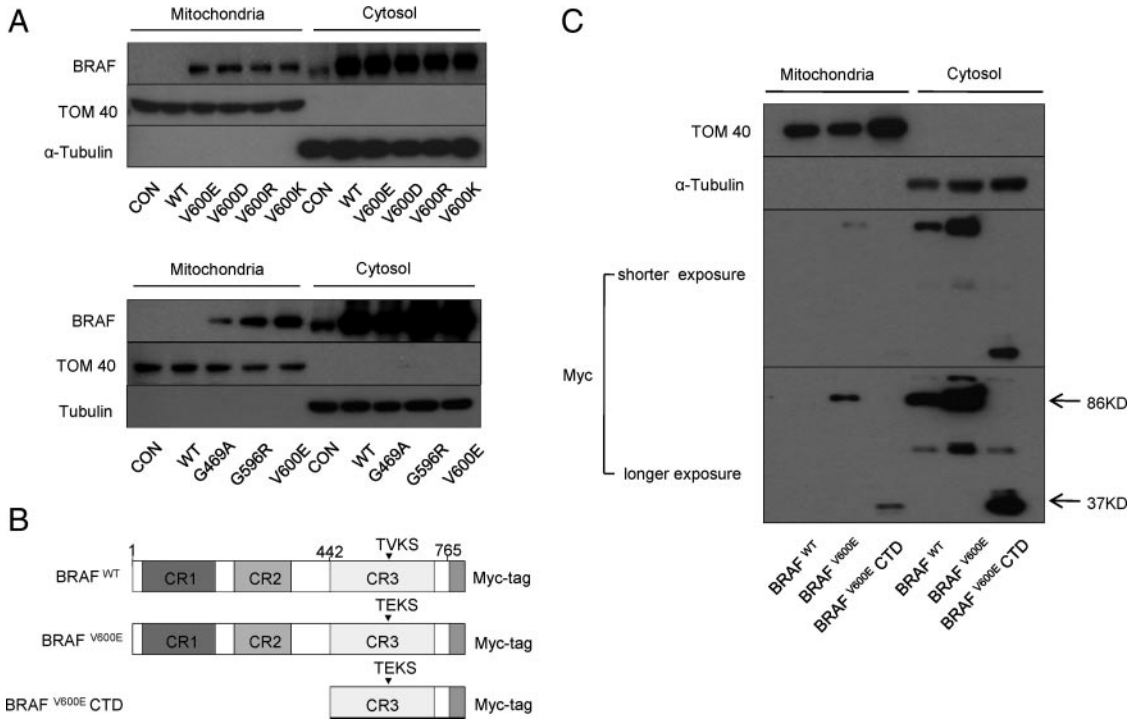

FIG. 2. Relationship between mutation-induced structural changes and mitochondrial translocation of $BRAF^{V600E}$. A, $PCCl_3$ cells were transiently transfected with the plasmid DNA indicated and incubated for 24 h in a CO_2 incubator. $PCCl_3$ cells were then prepared for subcellular fractionation. B, Schematic view of deletion constructs. Deletion constructs of $BRAF^{V600E}$ carrying the CR3 domain-containing C-terminal region ($BRAF^{V600E}$-CTD) were generated. C, HeLa cells were transiently transfected with the plasmid DNA indicated and incubated for 24 h. Full-length $BRAF^{V600E}$ was detected by Western blotting as an 86-kDa protein and the deletion construct of $BRAF^{V600E}$ was detected as a 37-kDa protein.

sequential digestion of the integral outer membrane protein TOM40, the inner membrane protein cytochrome *c* oxidase subunit IV, and then the matrix protein manganese superoxide dismutase revealed that $BRAF^{V600E}$ was digested in the same time point as TOM40. These experiments indicate $BRAF^{V600E}$ is associated with the outer membrane of mitochondria in thyroid cancer cells.

The above three experimental approaches suggest that $BRAF^{V600E}$ has a greater tendency than wild-type BRAF to localize to the outer membrane of mitochondria. Therefore, we speculate that $BRAF^{V600E}$ has direct roles to play in the mitochondrial outer membrane, which contains proteins regulating apoptosis and metabolic functions of mitochondria.

The C-terminal region of $BRAF^{V600E}$ is required for mitochondrial localization

The $BRAF^{V600E}$ mutation is located adjacent to the DFG motif and accounts for 90% of all BRAF mutations discovered in human cancers to date (5, 6). According to a computational model, the substitution of Glu for Val at residue 600 in BRAF ($BRAF^{V600E}$) induces structural changes that result in a larger pocket adjacent to the ATP-binding region (Supplemental Fig. 5A). The other constitutively active substitution mutants, *i.e.* $BRAF^{V600D}$, $BRAF^{V600K}$, and $BRAF^{V600R}$, also showed enlarged pockets similar to $BRAF^{V600E}$. Given the structural similarity and biological activity of these mutants, it was hypothesized that the other constitutively active mutants ($BRAF^{V600D}$, $BRAF^{V600K}$, and $BRAF^{V600R}$) could also localize to the mitochondria. As expected, a significant portion of $BRAF^{V600D}$, $BRAF^{V600K}$, and $BRAF^{V600R}$ proteins were observed in mitochondrial fractions, similar to $BRAF^{V600E}$ (Fig. 2A, upper panel). To reinforce structure-function studies using oncogenic BRAF mutants, we observed mitochondrial localization of other oncogenic BRAF mutants, $BRAF^{G469A}$ (BRAF mutants targeting P-loop) and $BRAF^{G596R}$ (oncogenic but impaired in BRAF kinase activity), which are predicted to have significant changes in their topography resulting in the formation of pocket-like structures (Supplemental Fig. 5, B and C). Both $BRAF^{G469A}$ and $BRAF^{G596R}$ mutant proteins were observed in the mitochondrial fraction (Fig 2A, *lower panel*).

These observations suggest that the interaction motif for mitochondrial localization is provided by the C-terminal region, which contains the CR3 domain. To verify this hypothesis, a deletion construct of $BRAF^{V600E}$ containing only the CR3 domain was generated (Fig. 2B). Interestingly, expression of the C-terminal domain of $BRAF^{V600E}$ was sufficient to induce the phosphorylation of MEK and ERK (data not shown) as well as for mitochondrial

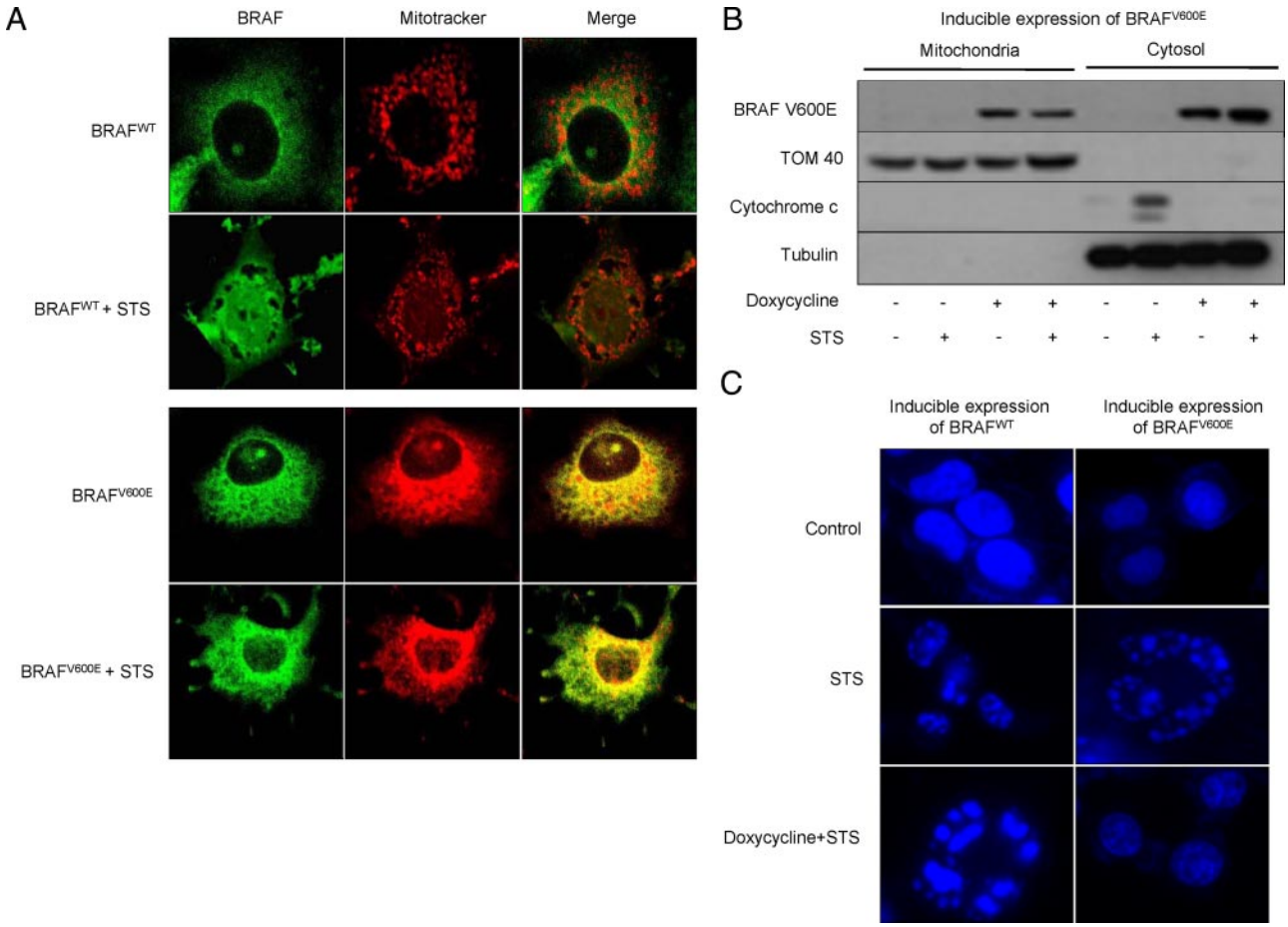

FIG. 3. Antiapoptotic effects of mitochondrial translocation of BRAF^{V600E}. A, HeLa-BRAF^{WT} and HeLa-BRAF^{V600E} treated with 1 μg doxycycline for 24 h were prepared and processed for immunofluorescence staining of BRAF (*green fluorescence*) and mitochondria (MitoTracker, *red fluorescence*), with or without STS (1 μM) treatment. B, HeLa-BRAF^{V600E} was prepared for subcellular fractionation with dimethylsulfoxide or STS treatment. C, HeLa-BRAF^{WT} and HeLa-BRAF^{V600E} were treated with STS and stained with 10 μL 4,6-diamidino-2-phenylindole mixture buffer in 1× PBS (10 ml) for 10 min at room temperature in the dark. Stained cells were observed under a fluorescence microscope.

localization (Fig. 2C). Taken together, these results indicate that mitochondrial localization is controlled by structural changes in the C-terminal region of mutants of BRAF.

Translocation of BRAF^{V600E} to the mitochondria generates resistance against mitochondrial apoptosis

To determine the role played by BRAF^{V600E}-specific mitochondrial localization, the differential susceptibilities of wild-type and mutant BRAF-containing cells to intrinsic apoptotic stimuli were compared. Hela cell lines expressing BRAF^{WT} or BRAF^{V600E} proteins in a doxycycline-inducible manner were generated for these experiments (HeLa-BRAF^{WT} and HeLa-BRAF^{V600E}, respectively; Supplemental Fig. 6). Although Hela cells are not thyroid malignant cells, they are widely used for mitochondrial research because they have characteristic mitochondrial properties, *e.g.* dynamic fusion and fission and biogenesis (22). Using these characteristics, we attempted to show the mitochondrial localization of mutant BRAF in Hela cells. The colocalization of BRAF with mitochondria was consistently observed in HeLa-BRAF^{V600E} (Fig. 3A), supporting the findings described above. HeLa-BRAF^{WT} displayed distinct apoptotic cellular changes such as extensive membrane blebbing and reduced cytoplasmic volume within 2 h of treatment with staurosporine (STS; 1 μM), a well-known inducer of apoptosis (Fig. 3A, *upper panel*). However, as shown in Fig. 3A (*bottom panel*), HeLa-BRAF^{V600E} was completely protected from STS-induced apoptotic processes and did not exhibit characteristic apoptotic cellular changes. Interestingly, these cells showed persistent translocation of BRAF^{V600E} to the mitochondria in the presence of STS.

To obtain additional evidence that BRAF^{V600E} confers apoptotic resistance, subcellular fractionation was performed to assess cytochrome *c* release to the cytoplasm in the presence or absence of STS. Mitochondrial cytochrome *c* is found as a dimer or tetramer; therefore, neither the monomeric nor the released forms of cytochrome *c*

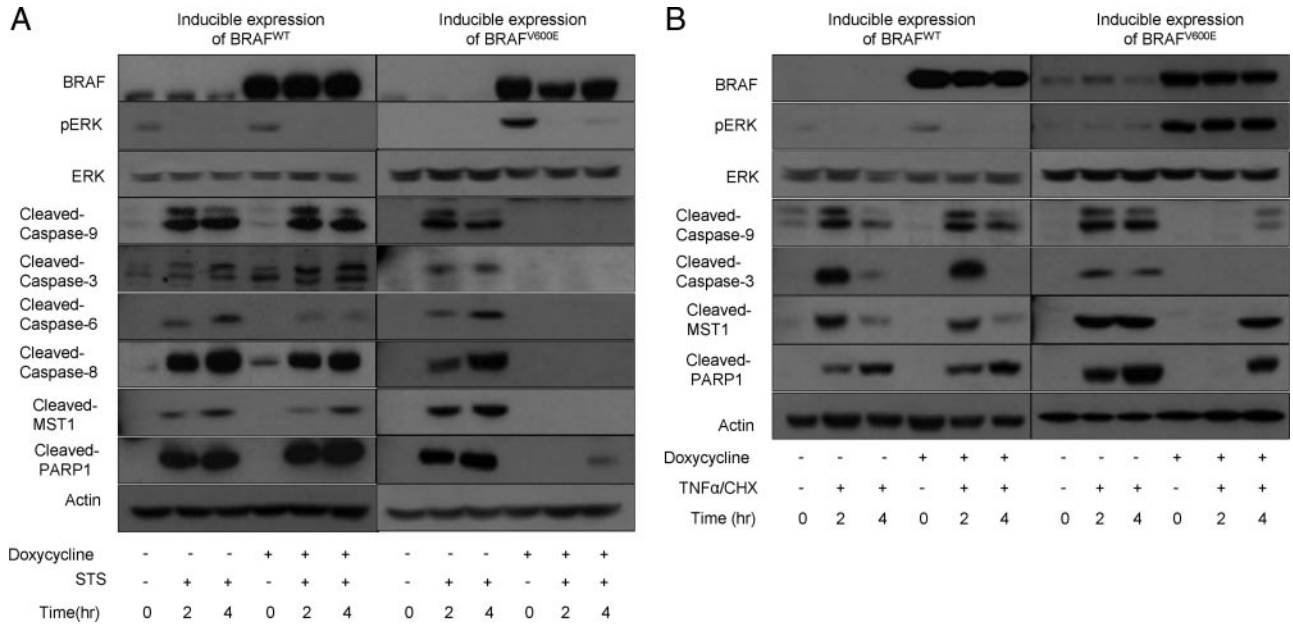

FIG. 4. Inhibition of caspase activation by mitochondrial localization of BRAF^{V600E}. A, After 24 h of 1 μg doxycycline treatment, HeLa-BRAF^{WT} and HeLa-BRAF^{V600E} were treated with dimethylsulfoxide (DMSO) or STS (1 μM) for the times indicated, and activation of the caspase system was analyzed by Western blotting. B, Doxycycline-treated HeLa-BRAF^{WT} and HeLa-BRAF^{V600E} were treated with DMSO or TNFα (50 ng/well) and CHX (10 μg/well) for the times indicated and analyzed by Western blotting.

were present in a nonreducing native SDS-PAGE of mitochondrial fractions (Fig. 3B). In the absence of BRAF^{V600E} expression, STS treatment showed a marked release of monomeric cytochrome *c* into the cytoplasm. However, induction of BRAF^{V600E} expression completely blocked the STS-mediated cytoplasmic release of cytochrome *c* (Fig. 3B). In a parallel experiment, STS treatment resulted in marked chromatin condensation in HeLa-BRAF^{WT}, but normal chromatin patterns were observed in HeLa-BRAF^{V600E} (Fig. 3B).

To investigate whether BRAF^{V600E} affected the activation of caspases or other executors of apoptosis, HeLa-BRAF^{WT} and HeLa-BRAF^{V600E} cells were treated with STS or TNFα/cycloheximide (CHX), and the cleavage of caspases, serine/threonine kinase 4 (MST1), and PARP was evaluated. After STS treatment, HeLa-BRAF^{WT} showed cleavage of caspases (caspase-9, -3, -6, -8), MST1, and PARP1. However, HeLa-BRAF^{V600E} did not show cleavage of caspases, MST1, or PARP1 after 4 h treatment with STS (Fig. 4A). TNFα/CHX treatment was strong enough to induce rapid apoptotic responses in cells containing BRAF^{WT}, which peaked around 2 h after the beginning of treatment. In HeLa-BRAF^{V600E}, the activation of caspase-9 and -3 was inhibited, and cleavage of MST1 and PARP was delayed in response to TNFα/CHX treatment (Fig. 4B). However, these inhibitory effects were modest in comparison with the STS resistance observed in the mutant cells. These results suggest that BRAF^{V600E} functions as an important modifier of apoptotic processes, especially in mitochondrial apoptosis; the translocation of BRAF^{V600E} to the mitochondria may be the mechanism underlying this apoptotic resistance.

Mitochondrial localization and antiapoptotic effects of BRAF^{V600E} were not blocked by BRAF or MEK inhibitors

Sorafenib was originally developed as an inhibitor of RAF kinase and is currently the focus of ongoing clinical trials that are targeting differentiated thyroid cancers (5). MEK inhibitors such as U0126 have also shown growth-inhibitory effects on BRAF^{V600E}-positive PTC (23). These inhibitors were therefore evaluated for their ability to block the mitochondrial localization of BRAF^{V600E}. Surprisingly, neither sorafenib (1 or 4 μM), nor U0126 (1 or 3 μM) altered or blocked the mitochondrial localization of BRAF^{V600E} (Fig. 5, A and B), even though these treatments were sufficient for marked or complete inhibition of MEK and ERK activation, respectively (Fig. 5, C and D). To verify the effect of the inhibitors on the localization of BRAF^{V600E} in thyroid cells, we performed transient transfection experiments using $PCCl_3$ cell lines and obtained consistent results (Supplemental Fig. 7). Based on these findings, it would appear that mitochondrial localization does not depend on BRAF^{V600E} activation of MEK or ERK.

The observation that the inhibition of MEK and ERK by sorafenib and U0126 did not alter the mitochondrial localization of BRAF^{V600E} indicates that these drugs do not play a role in mitochondrial apoptosis. U0126 and sorafenib effectively inhibited the phosphorylation

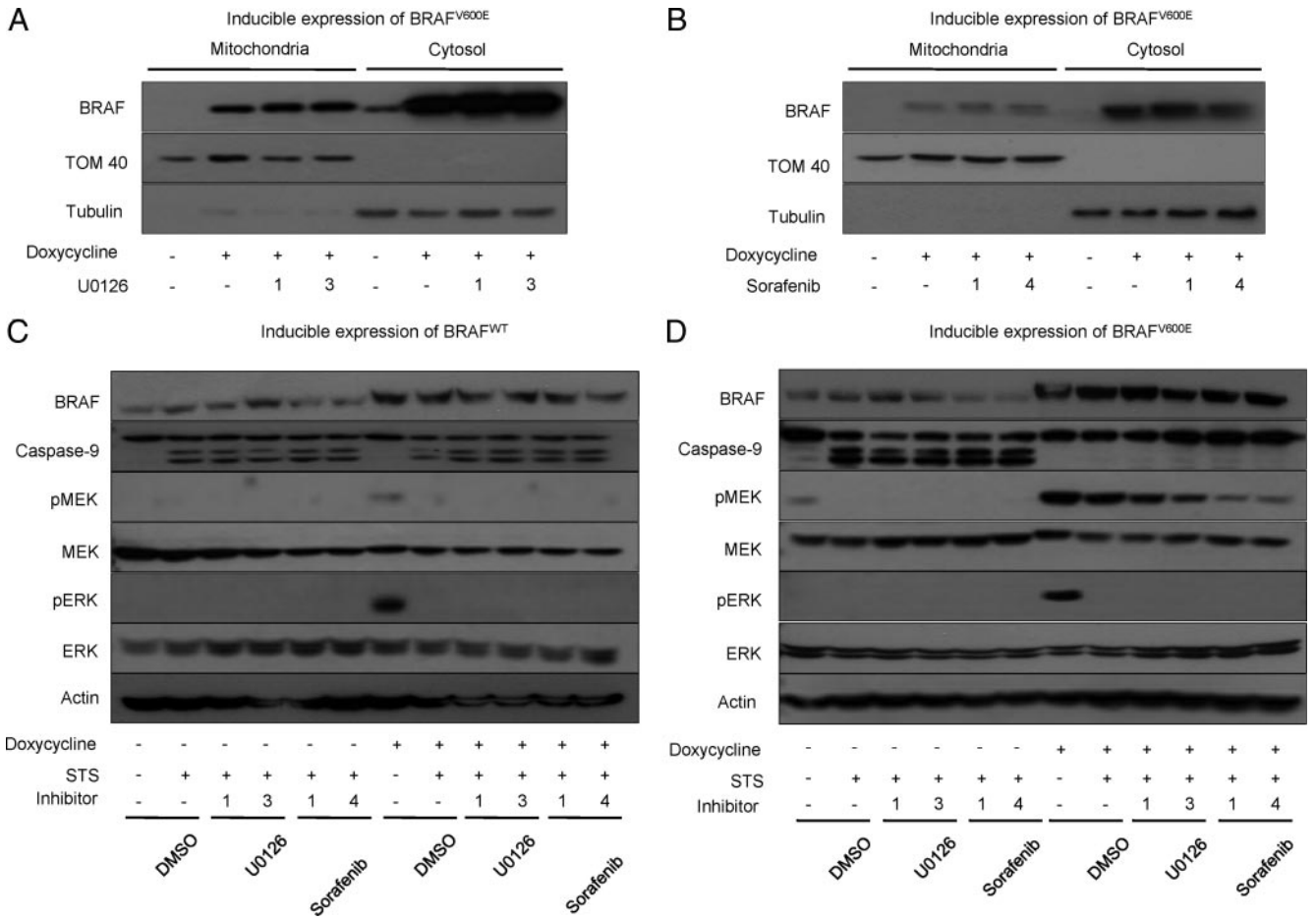

FIG. 5. Effect of U0126 and sorafenib on translocation of BRAF^{V600E} to mitochondria. A and B, HeLa-BRAF^{V600E} cells were treated for 4 h with the indicated concentrations of U0126 (A) or sorafenib (B) and then subjected to subcellular fractionation and immunoblot analysis. C and D, HeLa-BRAF^{WT} (C) and HeLa-BRAF^{V600E} (D) were treated for 4 h with the indicated concentrations of STS, U0126, or sorafenib and then analyzed by Western blotting. Before performing experiments, HeLa-BRAF^{WT} and HeLa-BRAF^{V600E} cells were treated with doxycycline and grown for 24 h in a humidified incubator (37 C, 5% CO_2). DMSO, Dimethylsulfoxide.

of MEK and ERK by both BRAF^{WT} and BRAF^{V600E}. Furthermore, STS treatment resulted in cleavage of caspase-9, regardless of the absence or presence of BRAF^{WT} (Fig. 5C). In contrast, BRAF^{V600E} expression provided protection against STS-mediated cleavage of caspase-9 (Fig. 5D) and this protection was not suppressed by treatment with U0126 or sorafenib. These observations indicate that the activation of MEK and ERK is not responsible for the anti-apoptotic effects and mitochondrial localization of BRAF^{V600E}. In the case of PLX4720, this BRAF^{V600E} selective inhibitor could not reverse the mitochondrial localization of BRAF^{V600E} or alleviate the protection against STS-induced caspase-9 cleavage (Supplementary Fig. 8).

BRAF^{V600E} is involved in high glycolytic activity and reduced mitochondrial oxidative phosphorylation

The mitochondrial localization of BRAF^{V600E} suggested that this protein might be responsible for certain changes in cellular energy metabolism observed in tumor cells such as aerobic glycolysis. The association between BRAF^{V600E} mitochondrial localization and glucose uptake, O_2 consumption and ATP generation was therefore examined using PC-BRAF^{WT} and PC-BRAF^{V600E}. Expression of BRAF^{WT} did not alter O_2 consumption, whereas expression of BRAF^{V600E} significantly suppressed O_2 consumption (Fig. 6A). Interestingly, inhibition of BRAF and MEK by sorafenib and U0126 did not reverse the suppression of O_2 consumption by BRAF^{V600E}. As shown in Fig. 6, B and C, inducible expression of BRAF^{V600E} markedly increased uptake of 2-deoxyglucose, and this increase was not affected by treatment with U0126 or sorafenib. There were no significant differences in the generation of ATP between PC-BRAF^{WT} and PC-BRAF^{V600E}, suggesting that in BRAF^{V600E} cells, higher glycolytic activities must be compensating for dysfunction in mitochondrial ATP generation. Taken together, these data suggested that BRAF^{V600E} modifies mito-

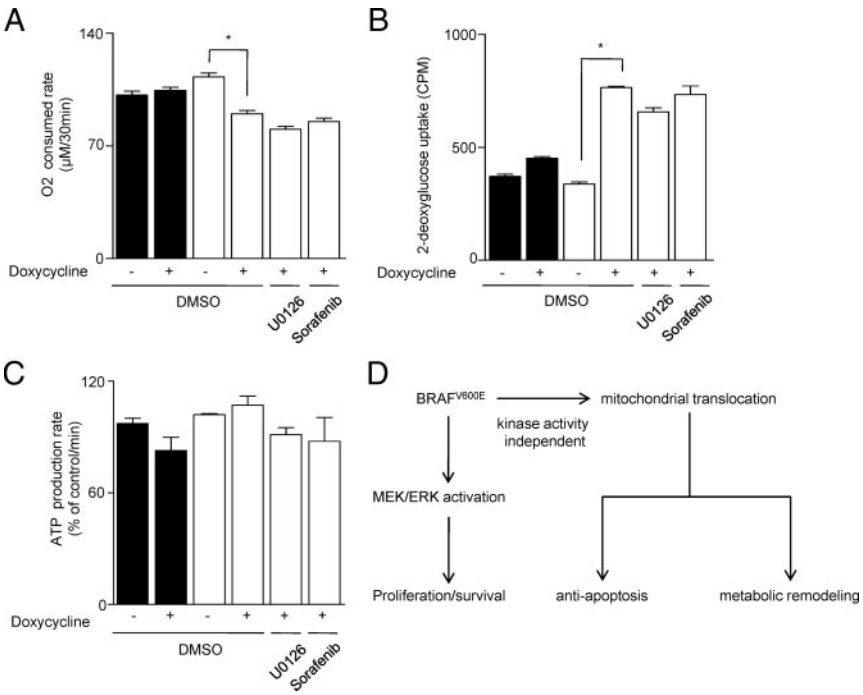

FIG. 6. Effects of $BRAF^{V600E}$ on mitochondrial energy metabolism. A–C, Concentration of O_2 consumed (A), glucose-uptake (B), and ATP production rate (C) in PC-$BRAF^{WT}$ and $BRAF^{V600E}$ are shown. PC-$BRAF^{WT}$ and $PCCl_3$-$BRAF^{V600E}$ were treated with doxycycline and grown for 48 h in a humidified incubator (37 C, 5% CO_2). *Black bars* represent PC-$BRAF^{WT}$ and *white bars* represent PC-$BRAF^{V600E}$. *P* values were calculated using the Mann-Whitney *U* test, and *asterisks* represent a statistically significant difference ($P < 0.05$). See *Materials and Methods* for a detailed description. D, A schematic representation of the experimental findings. $BRAF^{V600E}$ induces MEK/ERK activation, which increases cell proliferation and survival. Concurrently, $BRAF^{V600E}$ moves to the mitochondrial outer membrane and generates antiapoptotic effects and metabolic remodeling via kinase-independent activity. DMSO, Dimethylsulfoxide.

chondrial metabolism through mutation-specific mitochondrial localization, and these effects are independent of its kinase activities (Fig. 6D).

Discussion

The findings of the present study provide evidence, for the first time, that $BRAF^{V600E}$ is localized to the outer membrane of mitochondria in thyroid cancer. Mitochondrial localization of $BRAF^{V600E}$ was demonstrated by subcellular fractionation and fluorescence imaging in PTC-$BRAF^{V600E}$, PC-$BRAF^{V600E}$, and Tg-$BRAF^{V600E}$ mice. The mutant protein $BRAF^{V600E}$ was predicted to localize to the outer membrane of mitochondria, which contains the permeability transition pore complex regulating apoptosis and ATP generation. The mitochondrial localization of $BRAF^{V600E}$ was mutation specific and did not require ERK kinase activity. In addition, mitochondrial localization was accompanied by antiapoptosis activity and decreased mitochondrial function.

Mitochondrial localization usually requires a characteristic MTS, which enables interaction between the targeted molecule and the mitochondrial TOM complex (21). $BRAF^{V600E}$ does not contain the predicted MTS, suggesting that it is not transported into the inner membrane or matrix of mitochondria (24–28). Protease digestion experiments indicated that $BRAF^{V600E}$ is associated with the outer membrane. Therefore, the structural changes caused by this mutation must represent a prerequisite for mitochondrial association. The computational topographic analysis revealed that the $BRAF^{V600E}$ mutation forms a much wider surface pocket near the ATP binding site than that found in wild-type BRAF. Interestingly, the other active BRAF mutants ($BRAF^{V600D}$, $BRAF^{V600K}$, and $BRAF^{V600R}$) showed similar structural changes and were able to localize to the mitochondria. Deletion experiments showed that the C-terminal half of $BRAF^{V600E}$, which contains the CR3 domain, was sufficient for the translocation of $BRAF^{V600E}$ to the mitochondria, supporting the prediction that mutation-specific structural changes in BRAF may result in modified interactions that promote mitochondrial localization. However, mutation-induced structural changes also affect kinase activity, and this close structure-function relationship makes it difficult to exclude a possible role for kinase activity in mitochondrial localization. In the present study, however, several findings indicate that the mitochondrial localization of $BRAF^{V600E}$ is primarily driven by mutation-specific structural changes. To reinforce the structure-function studies, we investigated two other oncogenic BRAF mutants: $BRAF^{G469A}$ and $BRAF^{G596R}$. $BRAF^{G469A}$ has high kinase activity caused by mutation in the P-loop, and $BRAF^{G596R}$ has impaired kinase activity but demonstrated abilities to develop cancer (5). Subcellular fractionation demonstrated that oncogenic $BRAF^{G469A}$ and $BRAF^{G596R}$ were localized to mitochondria. In summary, oncogenic BRAF mutants with structural abnormalities in the CR3 region that do not affect their kinase activities may acquire the ability to localize to mitochondria, thereby providing kinase-dependent/-independent mitochondrial regulation of the development of thyroid cancer. Indeed, suppression of MEK and ERK activity by inhibitors such as sorafenib did not prohibit mitochondrial localization of $BRAF^{V600E}$. If the interaction between $BRAF^{V600E}$ and

mitochondrial proteins is mediated by structure, it is possible that small molecule inhibitors are not big enough to block large surface interactions.

In the present study, BRAF^{V600E} cells were shown to be resistant to intrinsic and extrinsic apoptotic stimuli, and the mitochondrial localization of BRAF^{V600E} was not affected by apoptotic stimuli. Previous studies performed on BRAF^{V600E}-positive melanoma cell lines have shown that its antiapoptotic effects were linked to constitutive MEK/ERK activation and therefore that disruption of MEK signaling pathways by inhibitors accelerated death in these cells. In melanoma cell models, the antiapoptotic functions of BRAF^{V600E} were explained by regulation of Bim, Bcl-2-associated death promoter (Bad), BCL-2, BCL-XL, and survivin in a MEK-dependent manner (29, 30). However, small interfering RNA silencing of Bim and Bad could not replicate the antiapoptotic effects of BRAF^{V600E} under the same experimental conditions (31). These results suggest that the antiapoptotic effects of BRAF^{V600E} are not entirely dependent on MEK/ERK signals. In our experimental model, a marked decrease in Bim stability was observed following BRAF^{V600E} induction, regardless of apoptotic stimuli. Bim protein levels were stabilized when MEK/ERK kinase activities were inhibited by U0126 and sorafenib, but reinduction of Bim did not confer any additional cleavage of caspase to oppose the antiapoptotic effect of BRAF^{V600E} (data not shown). Therefore, BRAF^{V600E} controls the expression of Bim via ERK activation, but its antiapoptotic effects are not dependent on the proapoptotic effects of Bim. The STS-treated apoptotic cells demonstrated marked cleavage of caspasep-9, which was accompanied by very low ERK activities in wild-type BRAF cells. However, STS-induced apoptosis is effectively suppressed in BRAF^{V600E} cells, which also have very low ERK activities. These findings suggest that ERK activation by BRAF^{V600E} may not be a critical factor determining the apoptotic responses. Taken together, these results suggest that the antiapoptotic effects of BRAF^{V600E} are not solely dependent on MEK/ERK activities in thyroid cells.

Sorafenib is currently applied to the treatment of advanced BRAF^{V600E}-positive melanoma and thyroid cancers. Because sorafenib showed effective inhibition of MEK and its downstream ERK kinase activities, its therapeutic focus was to induce cell death by inhibiting the kinase activities of BRAF^{V600E}. However, patients with BRAF^{V600E}-positive cancers did not achieve significant complete or partial remission when treated with sorafenib alone (7–9). This clinical failure may have resulted from resistance to cell death. The present findings that sorafenib failed to block the mitochondrial localization of BRAF^{V600E} and its antiapoptotic effects could provide insight into the molecular basis for the poor efficacy of sorafenib monotherapy for advanced thyroid cancer.

Metabolic remodelings are common phenomena in cancers, which often feature elevated glycolytic activity and suppression of mitochondrial OXPHOS function (16). Such characteristic metabolic changes enable the use of ^{18}F-fluorodeoxyglucose positron emission tomography/computed tomography for the diagnosis of PTC. Therefore, it is possible that BRAF^{V600E} contributes to or determines these characteristic metabolic changes in thyroid cancer. In this study, PC-BRAF^{V600E} showed a marked decrease in O_2 consumption and increased uptake of 2-deoxyglucose and generated a similar amount of overall ATP as control cell lines. These data indicate that BRAF^{V600E} is able to decrease mitochondrial ATP generation, but it compensates for overall ATP generation through an increase in glycolytic activity. In a previous study, BRAF^{V600E} was found to affect cellular levels of hypoxia-inducible factor (HIF)-1α, which is a well-known master regulator of hypoxia-induced vascular endothelial growth factor secretion (32). In addition to increased vascular endothelial growth factor expression, HIF1α induces a higher rate of glycolysis, generating the Warburg effect (33–35). However, with the exception of HIF1α, there has been little investigation into the alterations to cellular energy metabolism caused by BRAF^{V600E}. In the present experiments, HIF1α protein levels were not altered by BRAF^{V600E} because the $PCCl_3$ cell lines were grown under conventional culture conditions and not in a hypoxic chamber (data not shown). Despite the normoxic conditions, BRAF^{V600E} effectively generated the glycolytic phenotype, which could not be reversed by U0126 or sorafenib. These findings support the hypothesis that the translocation of BRAF^{V600E} to the mitochondria is important for its ability to generate emergent metabolic remodeling via a kinase-independent mechanism.

In summary, although we could not identify the interacting molecule(s) in the outer membrane, which would provide further evidence for a link between mitochondria and BRAF^{V600E}, the present findings revealed mitochondrial localization of BRAF^{V600E}. This observation supports plausible roles for BRAF^{V600E} in antiapoptosis and in the enhanced glycophenotypes associated with suppressed oxidative phosphorylation, which are common signature features of cancer cells. Surprisingly, none of these phenomena were affected by inhibitors of MEK or BRAF such as U0126 and sorafenib. Taken together, these data suggest that current clinically used BRAF^{V600E} inhibitors effectively inhibit BRAF^{V600E} kinase activity, but they do not block mitochondrial localization or the subcellular oncogenic activities of BRAF^{V600E}. In the future, it will be useful to determine the precise mechanisms

underlying translocation of $BRAF^{V600E}$ to the mitochondria because these MEK-ERK-independent subcellular effects of $BRAF^{V600E}$ represent a novel therapeutic target for patients with PTC resistant to MEK or BRAF kinase inhibitors.

Acknowledgments

We thank Dr. James A. Fagin (Memorial Sloan Kettering Cancer Center, New York, NY) for $PCCl_3$ cells with doxycycline-inducible expression of $BRAF^{V600E}$ and also acknowledge Bayer Schering Pharma AG (Berlin, Germany) for sorafenib. pEFm-$BRAF^{WT}$, -$BRAF^{V600E}$, -$BRAF^{V600D}$, -$BRAF^{V600R}$, and -$BRAF^{V600K}$ were kindly provided by Dr. Richard Marais and Dr. Robert Hayward (Institute of Cancer Research, London, UK). Homology modeling and computational assessments were performed by the Korean BioInformation Center (Daejeon, Korea, http://www.kobic.kr).

Address all correspondence and requests for reprints to: Minho Shong, M.D., Ph.D., Department of Internal Medicine, Chungnam National University School of Medicine, 640 Daesadong, Chungku Daejeon 301-721, Korea. E-mail: minhos@cnu.ac.kr; or Young Suk Jo, M.D., Ph.D., Research Center for Endocrine and Metabolic Diseases, Chungnam National University Hospital, 33 Munhwa-ro, Jung-gu Daejeon, 301-721, Korea. E-mail: ysmrj@cnuh.co.kr.

This work was supported by the National Research Foundation (NRF)/Ministry of Education, Science, and Technology (MEST) (Grant 2007-2003846/Grant 2007-2004079). M.H.L., S.E.L., M.J.R., S.J.K., Y.K.K., J.H.P., G.R.K., J.M.K., Y.S.J., and M.S. were supported in part by the second phase of the Brain Korea 21 Program/MEST. Y.S.J. was supported by NRF/MEST (Grant 2009-0077441).

Disclosure Summary: The authors have nothing to disclose.

References

1. **Davies H, Bignell GR, Cox C, Stephens P, Edkins S, Clegg S, Teague J, Woffendin H, Garnett MJ, Bottomley W, Davis N, Dicks E, Ewing R, Floyd Y, Gray K, Hall S, Hawes R, Hughes J, Kosmidou V, Menzies A, Mould C, Parker A, Stevens C, Watt S, Hooper S, Wilson R, Jayatilake H, Gusterson BA, Cooper C, Shipley J, Hargrave D, Pritchard-Jones K, Maitland N, Chenevix-Trench G, Riggins GJ, Bigner DD, Palmieri G, Cossu A, Flanagan A, Nicholson A, Ho JW, Leung SY, Yuen ST, Weber BL, Seigler HF, Darrow TL, Paterson H, Marais R, Marshall CJ, Wooster R, Stratton MR, Futreal PA** 2002 Mutations of the BRAF gene in human cancer. Nature 417:949–954
2. **Cohen Y, Xing M, Mambo E, Guo Z, Wu G, Trink B, Beller U, Westra WH, Ladenson PW, Sidransky D** 2003 BRAF mutation in papillary thyroid carcinoma. J Natl Cancer Inst 95:625–627
3. **Kimura ET, Nikiforova MN, Zhu Z, Knauf JA, Nikiforov YE, Fagin JA** 2003 High prevalence of BRAF mutations in thyroid cancer: genetic evidence for constitutive activation of the RET/PTC-RAS-BRAF signaling pathway in papillary thyroid carcinoma. Cancer Res 63:1454–1457
4. **Jo YS, Li S, Song JH, Kwon KH, Lee JC, Rha SY, Lee HJ, Sul JY, Kweon GR, Ro HK, Kim JM, Shong M** 2006 Influence of the BRAF V600E mutation on expression of vascular endothelial growth factor in papillary thyroid cancer. J Clin Endocrinol Metab 91:3667–3670
5. **Wan PT, Garnett MJ, Roe SM, Lee S, Niculescu-Duvaz D, Good VM, Jones CM, Marshall CJ, Springer CJ, Barford D, Marais R** 2004 Mechanism of activation of the RAF-ERK signaling pathway by oncogenic mutations of B-RAF. Cell 116:855–867
6. **Wellbrock C, Karasarides M, Marais R** 2004 The RAF proteins take centre stage. Nat Rev Mol Cell Biol 5:875–885
7. **Eisen T, Ahmad T, Flaherty KT, Gore M, Kaye S, Marais R, Gibbens I, Hackett S, James M, Schuchter LM, Nathanson KL, Xia C, Simantov R, Schwartz B, Poulin-Costello M, O'Dwyer PJ, Ratain MJ** 2006 Sorafenib in advanced melanoma: a Phase II randomised discontinuation trial analysis. Br J Cancer 95:581–586
8. **Gupta-Abramson V, Troxel AB, Nellore A, Puttaswamy K, Redlinger M, Ransone K, Mandel SJ, Flaherty KT, Loevner LA, O'Dwyer PJ, Brose MS** 2008 Phase II trial of sorafenib in advanced thyroid cancer. J Clin Oncol 26:4714–4719
9. **Kloos RT, Ringel MD, Knopp MV, Hall NC, King M, Stevens R, Liang J, Wakely Jr PE, Vasko VV, Saji M, Rittenberry J, Wei L, Arbogast D, Collamore M, Wright JJ, Grever M, Shah MH** 2009 Phase II trial of sorafenib in metastatic thyroid cancer. J Clin Oncol 27:1675–1684
10. **Adjei AA, Cohen RB, Franklin W, Morris C, Wilson D, Molina JR, Hanson LJ, Gore L, Chow L, Leong S, Maloney L, Gordon G, Simmons H, Marlow A, Litwiler K, Brown S, Poch G, Kane K, Haney J, Eckhardt SG** 2008 Phase I pharmacokinetic and pharmacodynamic study of the oral, small-molecule mitogen-activated protein kinase kinase 1/2 inhibitor AZD6244 (ARRY-142886) in patients with advanced cancers. J Clin Oncol 26:2139–2146
11. **Rinehart J, Adjei AA, Lorusso PM, Waterhouse D, Hecht JR, Natale RB, Hamid O, Varterasian M, Asbury P, Kaldjian EP, Gulyas S, Mitchell DY, Herrera R, Sebolt-Leopold JS, Meyer MB** 2004 Multicenter phase II study of the oral MEK inhibitor, CI-1040, in patients with advanced non-small-cell lung, breast, colon, and pancreatic cancer. J Clin Oncol 22:4456–4462
12. **Heidorn SJ, Milagre C, Whittaker S, Nourry A, Niculescu-Duvas I, Dhomen N, Hussain J, Reis-Filho JS, Springer CJ, Pritchard C, Marais R** 2010 Kinase-dead BRAF and oncogenic RAS cooperate to drive tumor progression through CRAF. Cell 140:209–221
13. **Hatzivassiliou G, Song K, Yen I, Brandhuber BJ, Anderson DJ, Alvarado R, Ludlam MJ, Stokoe D, Gloor SL, Vigers G, Morales T, Aliagas I, Liu B, Sideris S, Hoeflich KP, Jaiswal BS, Seshagiri S, Koeppen H, Belvin M, Friedman LS, Malek S** 2010 RAF inhibitors prime wild-type RAF to activate the MAPK pathway and enhance growth. Nature 464:431–435
14. **Cichowski K, Jänne PA** 2010 Drug discovery: inhibitors that activate. Nature 464:358–359
15. **Knauf JA, Fagin JA** 2009 Role of MAPK pathway oncoproteins in thyroid cancer pathogenesis and as drug targets. Curr Opin Cell Biol 21:296–303
16. **Ashrafian H** 2006 Cancer's sweet tooth: the Janus effect of glucose metabolism in tumorigenesis. Lancet 367:618–621
17. **Kim JW, Dang CV** 2006 Cancer's molecular sweet tooth and the Warburg effect. Cancer Res 66:8927–8930
18. **Moretti S, De Falco V, Tamburrino A, Barbi F, Tavano M, Avenia N, Santeusanio F, Santoro M, Macchiarulo A, Puxeddu E** 2009 Insights into the molecular function of the inactivating mutations of B-Raf involving the DFG motif. Biochim Biophys Acta 1793:1634–1645
19. **Mitsutake N, Knauf JA, Mitsutake S, Mesa Jr C, Zhang L, Fagin JA** 2005 Conditional BRAFV600E expression induces DNA synthesis, apoptosis, dedifferentiation, and chromosomal instability in thyroid PCCL3 cells. Cancer Res 65:2465–2473
20. **Knauf JA, Ma X, Smith EP, Zhang L, Mitsutake N, Liao XH, Refetoff S, Nikiforov YE, Fagin JA** 2005 Targeted expression of BRAFV600E in thyroid cells of transgenic mice results in papillary

thyroid cancers that undergo dedifferentiation. Cancer Res 65: 4238–4245
21. **Neupert W, Herrmann JM** 2007 Translocation of proteins into mitochondria. Annu Rev Biochem 76:723–749
22. **Detmer SA, Chan DC** 2007 Functions and dysfunctions of mitochondrial dynamics. Nat Rev Mol Cell Biol 8:870–879
23. **Liu D, Hu S, Hou P, Jiang D, Condouris S, Xing M** 2007 Suppression of BRAF/MEK/MAP kinase pathway restores expression of iodide-metabolizing genes in thyroid cells expressing the V600E BRAF mutant. Clin Cancer Res 13:1341–1349
24. **Small I, Peeters N, Legeai F, Lurin C** 2004 Predotar: a tool for rapidly screening proteomes for N-terminal targeting sequences. Proteomics 4:1581–1590
25. **Guda C, Fahy E, Subramaniam S** 2004 MITOPRED: a genome-scale method for prediction of nucleus-encoded mitochondrial proteins. Bioinformatics 20:1785–1794
26. **Emanuelsson O, Nielsen H, Brunak S, von Heijne G** 2000 Predicting subcellular localization of proteins based on their N-terminal amino acid sequence. J Mol Biol 300:1005–1016
27. **Claros MG** 1995 MitoProt, a Macintosh application for studying mitochondrial proteins. Comput Appl Biosci 11:441–447
28. **Nakai K, Horton P** 1999 PSORT: a program for detecting sorting signals in proteins and predicting their subcellular localization. Trends Biochem Sci 24:34–36
29. **Boisvert-Adamo K, Aplin AE** 2008 Mutant B-RAF mediates resistance to anoikis via Bad and Bim. Oncogene 27:3301–3312
30. **Hilmi C, Larribere L, Giuliano S, Bille K, Ortonne JP, Ballotti R, Bertolotto C** 2008 IGF1 promotes resistance to apoptosis in melanoma cells through an increased expression of BCL2, BCL-X(L), and survivin. J Invest Dermatol 128:1499–1505
31. **Sheridan C, Brumatti G, Martin SJ** 2008 Oncogenic B-RafV600E inhibits apoptosis and promotes ERK-dependent inactivation of Bad and Bim. J Biol Chem 283:22128–22135
32. **Kumar SM, Yu H, Edwards R, Chen L, Kazianis S, Brafford P, Acs G, Herlyn M, Xu X** 2007 Mutant V600E BRAF increases hypoxia inducible factor-1α expression in melanoma. Cancer Res 67:3177–3184
33. **DeBerardinis RJ, Lum JJ, Hatzivassiliou G, Thompson CB** 2008 The biology of cancer: metabolic reprogramming fuels cell growth and proliferation. Cell Metab 7:11–20
34. **Maxwell PH** 2005 Hypoxia-inducible factor as a physiological regulator. Exp Physiol 90:791–797
35. **Maxwell PH** 2005 The HIF pathway in cancer. Semin Cell Dev Biol 16:523–530